Geo-Mar Lett (2012) 32:29–37
DOI 10.1007/s00367-011-0236-0

ORIGINAL

Wave friction factor rediscovered

J. P. Le Roux

Received: 4 November 2010 / Accepted: 31 March 2011 / Published online: 19 April 2011

Abstract The wave friction factor is commonly expressed as a function of the horizontal water particle semi-excursion (A_{wb}) at the top of the boundary layer. A_{wb}, in turn, is normally derived from linear wave theory by $\frac{U_{wb}T_w}{2\pi}$, where U_{wb} is the maximum water particle velocity measured at the top of the boundary layer and T_w is the wave period. However, it is shown here that A_{wb} determined in this way deviates drastically from its real value under both linear and non-linear waves. Three equations for smooth, transitional and rough boundary conditions, respectively, are proposed to solve this problem, all three being a function of U_{wb}, T_w, and δ, the thickness of the boundary layer. Because these variables can be determined theoretically for any bottom slope and water depth using the deepwater wave conditions, there is no need to physically measure them. Although differing substantially from many modern attempts to define the wave friction factor, the results coincide with equations proposed in the 1960s for either smooth or rough boundary conditions. The findings also confirm that the long-held notion of circular water particle motion down to the bottom in deepwater conditions is erroneous, the motion in fact being circular at the surface and elliptical at depth in both deep and shallow water conditions, with only horizontal motion at the top of the boundary layer. The new equations are incorporated in an updated version (WAVECALC II) of the Excel program published earlier in this journal by Le Roux et al. Geo-Mar Lett 30(5): 549–560, (2010).

Electronic supplementary material The online version of this article (doi:10.1007/s00367-011-0236-0) contains supplementary material, which is available to authorized users.

J. P. Le Roux (✉)
Departamento de Geología, Facultad de Ciencias Físicas y Matemáticas, Universidad de Chile,
Casilla 13518, Correo 21,
Santiago, Chile
e-mail: jroux@cec.uchile.cl

Introduction

Sediment transport in the marine environment is usually the result of both wave and current action. The total shear stress τ_t exerted on the bottom by these two processes can be expressed as

$$\tau_t = \tau_u + \tau_w \quad (1)$$

where the subscripts u and w indicate current- and wave-induced stress, respectively. τ_u and τ_w must be computed in the same manner to be compatible (Le Roux 2003), but whereas τ_u is calculated from measured velocity profiles, τ_w is commonly derived from the maximum horizontal water particle velocity at the top of the boundary layer (henceforth referred to as the boundary velocity U_{wb}) using the quadratic friction law

$$\tau_w = 0.5\rho f_w {U_{wb}}^2 \quad (2)$$

where ρ is the water density and f_w the wave friction factor, a dimensionless parameter.

Unfortunately, f_w has always been somewhat of an enigma, with numerous attempts to define it leading to widely discrepant results (Soulsby and Whitehouse 1997). One of the problems has been that the boundary layer was poorly understood in terms of both its thickness and velocity profile (Teleki 1972). A further problem is that sediments are entrained by two processes acting simultaneously under waves, one related to the oscillatory shear stress τ_w, which is a direct function of the wave friction

factor as shown in Eq. 2, and an additional force due to the horizontal pressure gradient across the grain, P_w. According to Soulsby and Whitehouse (1997), P_w is in quadrature with the shear stress and has an increasing effect with an increase in grain size. The net force under waves is thus greater than the shear stress alone, at least under rough boundary conditions (Le Roux 2010a).

Recent developments in wave modeling (see Le Roux et al. 2010, and references therein; Le Roux 2010a, b) have now made it possible to resolve these parameters, which allow a more refined analysis of the friction factor. To carry out this study, the WAVECALC program of Le Roux et al. (2010) was used, of which an updated version (WAVECALC II) is available online in the electronic supplementary material. Due to the fact that numerous calculations are required to arrive at the results reported here, only the most relevant equations are shown in the text below. Those pertaining to sediment transport are presented in Appendix 1 (see Le Roux 1992, 1998), together with a list of symbol definitions (Appendix 2). Other equations used in wave modeling can be derived from WAVECALC II.

Methods

Hydraulic condition of the wave boundary layer

From early on, it was recognized that the wave friction factor is different under hydraulically smooth (laminar) and rough (turbulent) boundary conditions, which depend on the Reynolds number $\mathrm{Re} = \frac{\rho L U}{\mu}$, where L is a length term, U a velocity term, and μ the dynamic water viscosity. However, the limit between these two conditions has been uncertain, because at least three different Reynolds numbers may be applicable. Komar and Miller (1973), for example, used the grain diameter D as the length term and U_{wb} as the velocity term, whereas Mirfenderesk and Young (2003) and many others replaced L with the water particle semi-excursion above the boundary layer, A_{wb}. Le Roux (2010b), on the other hand, demonstrated that the boundary Reynolds number $\mathrm{Re}_{*c} = \frac{\rho D U_{*c}}{\mu}$, where U_{*c} is the critical shear velocity required to entrain sediments under unidirectional currents (Eqs. 1–5 in Appendix 1), is well suited to distinguish between different hydraulic conditions in the wave boundary layer. This is also followed here.

Different ways to determine f_w

The wave friction factor can be determined in three ways. The first is by direct measurement using a bottom-mounted shear plate to obtain τ_w, which together with direct measurement of U_{wb} can be used in Eq. 2 to calculate f_w (Mirfenderesk and Young 2003). As pointed out by Mirfenderesk and Young (2003), however, this method is complicated and demanding, needing careful corrections to remove spurious edge forces exerted on the plate. It can be added that the wave friction factor for loose sediments would also be different from that obtained by gluing sand to a shear plate.

The second method is to measure the velocity profile within the boundary layer with a laser Doppler anemometer (Mirfenderesk and Young 2003). This involves solving the linearized momentum equation for the flow, $\rho \frac{\partial}{\partial_t}(U_{wi} - U_{wb}) = \frac{\partial \tau_w}{\partial_{zb}}$ where zb is the vertical coordinate measured upward from the bed, and U_{wi} is the instantaneous velocity. This equation contains two unknowns, U_{wi} and τ_w, for which either a drag law model (Eq. 2) or an eddy viscosity model can be used to parameterize τ_w and obtain closure. In the eddy viscosity model, the shear stress is parameterized in terms of the velocity gradient in the bottom boundary layer, where $\tau_w = \upsilon_t \left(\frac{\partial U_{wi}}{\partial_{zb}}\right)$ in which υ_t is the turbulent eddy viscosity. The main problem in solving this equation involves the way in which the eddy viscosity is modeled, some authors using a time-variant eddy viscosity (Trowbridge and Madsen 1984a, b) and others a time-invariant viscosity (You et al. 1992; Hsu and Ou 1997), which differ in the way they describe the eddy viscosity distribution within the boundary layer. Alternatively, higher-order turbulent closure schemes can be used to model the turbulent field within the wave boundary layer (Justesen 1988; Aydin and Shuto 1998).

The method proposed in this paper relates sediment entrainment under waves to the numerous experimental studies on sediment entrainment thresholds under unidirectional currents. Le Roux (1998) showed that the Shields (1936) dimensionless critical shear stress τ_{dc} under such currents can be calculated from the dimensionless settling velocity W_d of the grains, which takes the grain size and density as well as water properties into account (Eq. 4 in Appendix 1). τ_{dc} can be related directly to the quadratic friction law (Le Roux 2003). At the moment of sediment entrainment by traction, the critical wave friction factor f_{wc} equals $\frac{\tau_{wc}}{0.5\rho U_{wbc}{}^2}$ (Eq. 2). Considering that $\tau_{wc} = \rho U_{*wc}{}^2$, where U_{*wc} is the critical wave boundary shear velocity under the wave crest,

$$f_{wc} = \frac{2\tau_{wc}}{\rho U_{wbc}{}^2} = \frac{2\rho U_{*wc}{}^2}{\rho U_{wbc}{}^2} = \frac{2U_{*wc}{}^2}{U_{wbc}{}^2} \quad (3)$$

The critical wave boundary shear velocity U_{*wc} at the moment of sediment entrainment can be determined using the following equations for smooth, transitional and rough

conditions, respectively (Le Roux 2010a): for smooth conditions ($Re_{*c}<3.7$)

$$U_{*wc} = 5.453 \times 10^{-2}\left(\frac{\rho D U_{*c}{}^2 H_o}{\mu d}\right)^{0.1630} \quad (4)$$

for transitional conditions ($3.7<Re_{*c}<65$)

$$U_{*wc} = 7.174 \times 10^{-3}\left(\frac{\rho D U_{*c}{}^2 H_o}{\mu \delta}\right)^{0.2001} \quad (5)$$

and for fully rough conditions ($Re_{*c}>65$)

$$U_{*wc} = 4.240 \times 10^{-3}\left(\frac{\rho D U_{*c}{}^2 H_o}{\mu \delta}\right)^{0.3630} \quad (6)$$

where H_o is the fully developed deepwater wave height, d the water depth, and δ the thickness of the boundary layer.

Although U_{wbc} or U_{wb} can be obtained for fully developed waves at any depth (Le Roux 2010b), U_{*wc} can only be derived for the moment of sediment entrainment as it requires U_{*c} (Eqs. 1–5 in Appendix 1). f_{wc} can therefore be calculated in this way, but it does not give a solution to f_w when sediment is not being entrained. A general relationship between f_w and the water and sediment properties, as well as the wave characteristics, must therefore be sought.

f_w as determined by dimensional analysis

The parameters most likely to be involved in the wave friction factor are U_{wb}, D, δ, ρ, μ, A_{wb}, the wave period T_w, and the water depth d. Because f_w is a dimensionless entity, these variables have to be arranged into a dimensionless group or groups, although not necessarily incorporating every parameter.

Many different dimensionless combinations can be tested against experimental data, in this case at the critical condition, to find the best correlation. Table 1 displays a wide variety of hypothetical wave conditions, water depths and sediment sizes. In column 12, the critical wave friction factor was calculated using Eq. 3, with U_{*c} based on numerous experimental data as summarized in Eqs. 1–5 of Appendix 1. This was plotted against various dimensionless groups.

Results

Equations for the wave friction factor

Using trial and error, the following equations were found to give good results for smooth, transitional and rough boundary conditions as defined in Eqs. 4–6 above. For smooth boundary conditions

$$f_w = 6.848 \times 10^{-3}\left(\frac{\mu^2 U_{wb} T_w}{g\rho^2 D\delta^3}\right)^{0.28} \quad (7)$$

with a coefficient of determination (R^2) of 0.9934.

For transitional boundary conditions

$$f_w = 0.1087\left(\frac{g\delta}{U_{wb}}\sqrt{\frac{\rho T_w}{\mu}}\right)^{-0.41} \quad (8)$$

where R^2 is 0.9713.

For rough boundaries

$$f_w = 2,715\left(\frac{D\delta^2}{dT_w{}^2 U_{wb}{}^2}\right) + 0.0054 \quad (9)$$

where R^2 is 0.9470.

Figure 1 compares the wave friction factor computed by Eqs. 7–9 against that of Eq. 3. However, instead of being limited to threshold conditions as in the case of Eq. 3, all the variables in Eqs. 7–9 can be obtained for sediments of different sizes in any fully developed wave condition and water depth.

Comparison with previous equations

Most methods to calculate f_w only distinguish between smooth and rough boundary conditions. One of the earliest equations for smooth conditions was that of Jonsson (1966), who proposed using $f_w = 2\sqrt{\frac{\mu}{0.5\rho U_{wb} d_{ob}}}$, where d_{ob} is the orbital diameter.

Shortly thereafter, Schlichting (1968) derived an equation from analytical evaluation: $f_w = \frac{2\left(\omega\frac{\mu}{\rho}\right)^{0.5}}{U_{wb}}$ where ω is the radian frequency $\frac{2\pi}{T_w}$. Both these authors assumed a circular orbit at the top of the boundary layer, so that $U_{wb} = \frac{\pi d_{ob}}{T_w}$. This resolves to the same equation, namely

$$f_w = \sqrt{\frac{8\mu T_w}{\pi\rho d_{ob}{}^2}} \quad (10)$$

More recently, Wang (2007) proposed a formula for all boundary conditions:

$$f_w = (0.407)^2\left[\frac{1}{\ln\left(\frac{A_{wb}}{2D}\right)}\right]^2 \quad (11)$$

Figure 2 compares the values obtained by Eqs. 7, 10 and 11 to those of Eq. 3. There is a reasonable, almost 1:1 correlation as shown by the regression lines of Eqs. 7 and 10, but with much less data scatter in the case of Eq. 7,

Table 1 Comparison of wave friction factors as determined in this paper with Jonsson (1963, 1966), Schlichting (1968), and Wang (2007)

T_w (s)	H_o (m)	D (m)	τ_{dc} (kg m^{-1} s^{-1})	U_{*c} (m s^{-1})	δ (m)	Re_{*c}	U_{wbc} (m s^{-1})	U_{*wc} (m s^{-1})	A_{wb} Eq. 15 (m)	A_{whz} Eq. 16 (m)	f_{wc} Eq. 3	f_w Eqs. 7-9	f_w Schlichting	f_w Wang
12.8098	9.0611	0.00001	0.2377	0.0061	0.00045	0.0632	*0.0845*	0.0094	0.1723	0.1646	0.0271	*0.0254*	0.0341	0.0047
9.6073	5.0968	0.00001	0.2377	0.0061	0.0003	0.0632	0.076	0.0095	0.1162	0.1137	0.0326	0.0324	0.0427	0.0052
6.4049	2.2653	0.00001	0.2377	0.0061	0.00015	0.0632	0.0605	0.0096	0.0617	0.0656	00444	00486	0.0604	0.0062
3.2024	0.5663	0.00001	0.2377	0.0061	0.00005	0.0632	0.0353	0.0098	0.018	0.0242	0.0851	0.0865	0.116	0.0089
12.8098	9.0611	0.000025	0.1805	0.0084	0.00045	0.2174	0.1201	0.0124	0.2449	0.2303	0.0241	0.022	00244	0.0054
9.6073	5.0968	0.000025	0.1805	0.0084	0.0003	0.2174	0.1086	0.0125	0.1661	*0.1589*	0.0289	0.0277	0.0306	0.006
6.4049	2.2653	0.000025	0.1805	0.0084	0.00015	0.2174	0.0879	0.0126	0.0896	0.0912	0.0396	0.0417	0.0435	0.0072
3.2024	0.5663	0.000025	0.1805	0.0084	0.00005	0.2174	0.0553	0.0129	0.0282	0.0335	0.0769	0.0759	0.0833	0.0104
12.8098	9.0611	0.00005	01376	0.0103	0.00045	0.5332	0.1524	0.015	0.3107	0.2971	0.0212	00193	00189	0.0061
9.6073	5.0968	0.00005	0.1376	0.0103	0.0003	0.5332	0.1384	0.0151	0.2116	0.2042	0.0255	0.0244	0.0238	0.0068
6.4049	2.2653	0.00005	0.1376	0.0103	0.00015	0.5332	0.1142	0.0153	0.1164	0.1171	0.0355	0.037	00338	0.0082
3.2024	0.5663	0.00005	0.1376	0.0103	0.00005	0.5332	0.0751	0.0157	0.0383	0.043	0.0694	0.0681	0.065	0.012
12.8098	9.0611	0.000075	0.1138	0.0115	0.00045	0.893	0.1742	0.0167	0.3551	0.3446	0.0195	0.0179	0.0163	0.0066
9.6073	5.0968	0.000075	0.1138	0.0115	0.0003	0.893	0.1596	0.0169	0.244	0.2367	0.0238	0.0227	0.0205	0.0074
6.4049	2.2653	0.000075	0.1138	0.0115	000015	0893	0.1324	0.0171	0.135	0.136	0.0331	00344	0.0292	0.0089
3.2024	0.5663	0.000075	0.1138	0.0115	0.00005	0.893	0.0884	0.0175	0.0451	0.0497	0.0646	0.0637	0.0561	0.0132
12.8098	9.0611	0.0001	0.0981	0.0124	0.00045	1.2838	0.1911	0.018	0.3896	0.383	0.0184	0.017	0.0146	0.007
9.6073	5.0968	0.0001	0.0981	0.0124	0.0003	1.2838	0.1753	0.0182	0.268	0.2628	0.0224	0.0215	0.0184	0.0078
6.4049	2.2653	0.0001	0.0981	0.0124	0.00015	1.2838	0.1469	0.0185	0.1497	0.2027	0.0315	0.0327	0.0194	0.0094
3.2024	0.5663	0.0001	0.0981	0.0124	0.00005	1.2838	0.0991	0.0189	0.0505	0.0550	0.0614	00606	0.0506	0.0141
6.4049	2.2653	0.000245	0.0548	0.0145	0.00015	3.6781	0.1951	0.023	0.1989	0.2027	0.0256	0.0275	0.0715	0.0117
12.8098	9.0611	0.00025	0.054	0.0145	0.00045	3.7532	0.2976	0.0291	0.6067	0.5354	0.0246	0.0212		0.0081
9.6073	5.0968	0.00025	0.054	0.0145	0.0003	3.7532	0.2589	0.0281	0.3959	0.3666	0.0275	0.0251		0.0093
6.4049	2.2653	000025	0054	0.0145	0.00015	3.7532	0.2057	0.0275	0.2097	0.2089	0M36	00329		0.0116
3.2024	0.5663	0.00025	0.054	0.0145	0.00475	3.7532	0.1676	0.0104	0.0854	0.0724	0.0097	0.0085		0.0168
12.8098	9.0611	0.0005	00354	0.0166	0.00055	8.5934	0.3554	0.0339	0.7246	0.6898	0M201	0021		0.0095
9.6073	5.0968	0.0005	0.0354	0.0166	0.0003	8.5934	0.3058	0.0341	0.4676	0.4711	0.0245	0.0268		0.0111
6.4049	2.2653	0.0005	0.0354	0.0166	0.00015	8.5934	0.2409	0.0333	0.2456	0.2677	0.0322	0.0351		0.0143
3.2024	0.5663	0.0005	0.0354	0.0166	0.01405	8.5934	0.1896	0.0102	0.0966	0.0834	0.0057	0.0057		0.022
12.8098	9.0611	0.00075	0.0387	0.0212	0.00055	16.4621	0.4119	0.0406	0.8398	0.8001	0.0214	0.0223		0.0104
9.6073	5.0968	0.00075	0.0387	0.0212	0.0003	16.4621	0.3521	0.0408	0.5384	0.5456	0.0262	0.0284		0.0123
6.4049	2.2653	0.00075	0.0387	0.0212	0.02155	16.4621	0.2859	0.0148	0.2914	0.2923	0.0047	0.0049		0.0158
3.2024	0.5663	0.00075	0.0387	0.0212	0.01945	16.4621	0.2173	0.0114	0.1108	0.0901	0.0053	0.0053		0.0254
12.8098	9.0611	0.001	0.0408	0.0252	0.00055	26.0909	0.4331	0.046	0.883	0.8885	0.0223	0.0227		0.0114
9.6073	5.0968	0.001	0.0408	0.0252	0.0014	26.0909	0.3996	0.034	0.611	0.6047	0.0147	0.0159		0.0131
6.4049	2.2653	0.001	0.0408	0.0252	0.03695	26.0909	0.299	0.015	0.3048	0.3103	0.004	0.004		0.0176
3.2024	0.5663	0.001	0.0408	0.0252	0.02325	26.0909	0.2347	0.0125	0.1196	0.0951	0.0052	0.0051	Jonsson	0.0287

6.4049	2.2653	0.0018	0.0444	0.0353	0.06845	65.7S64	0.359	0.0204	0.366	0.1555	0.0048	0.0057	0.0066	0.0215
12.8098	9.0611	0.0025	0.045	0.0418	0.08725	108.1944	0.6831	0.0393	1.3927	1.1704	0.0083	0.0054	0.0066	0.0136
9.6073	5.0968	0.0025	0.045	0.0418	0.1125	108.1944	0.5243	0.0291	0.8017	0.7335	0.0056	0.0055	0.0062	0.0172
6.4049	2.2653	0.0025	0.045	0.0418	0.08605	108.1944	0.4146	0.0239	0.4226	0.3713	0.0052	0.0059	0.0066	0.0236
3.2024	0.5663	0.0025	0.045	0.0418	0.03535	108.1944	0.3025	0.02	0.1542	0.1114	0.0069	0.0084	0.0087	0.0443
12.8098	9.0611	0.005	0.045	0.0592	0.23825	306.4646	0.8208	0.0452	1.6734	1.3509	0.0067	0.0055	0.0061	0.0169
9.6073	5.0968	0.005	0.045	0.0592	0.1969	306.4646	0.6949	0.0393	1.0625	0.8395	0.0062	0.0057	0.0064	0.021
6.4049	2.2653	0.005	0.045	0.0592	0.12315	306.4646	0.5729	0.0347	0.584	0.4203	0.0067	0.0066	0.0073	0.0291
3.2024	0.5663	0.005	0.045	0.0592	0.04445	306.4646	0.4245	0.0304	0.2164	0.1239	0.0098	0.011	0.0103	0.0584
12.8098	9.0611	0.0075	0.045	0.0724	0.36125	562.197	0.9475	0.0521	1.9317	1.5071	0.0059	0.0057	0.006	0.0191
9.6073	5.0968	0.0075	0.045	0.0724	0.2502	562.197	0.8341	0.0483	1.2754	0.9097	0.0068	0.006	0.0067	0.0236
6.4049	2.2653	0.0075	0.045	0.0724	0.14455	562.197	0.6979	0.0439	0.7114	0.4497	0.008	0.0072	0.0079	0.0331
3.2024	0.5663	0.0075	0.045	0.0724	0.04955	562.197	0.5182	0.0392	0.2641	0.1312	0.0122	0.0132	0.0114	0.07
12.8098	9.0611	0.01	0.045	0.0837	0.44795	866.5909	1.0695	0.0594	2.1804	1.6215	0.0057	0.0059	0.0062	0.0207
9.6073	5.0968	0.01	0.045	0.0837	0.3004	866.5909	0.9473	0.0557	1.4485	0.9775	0.0067	0.0064	0.0069	0.0257
6.4049	2.2653	0.01	0.045	0.0837	0.15975	866.5909	0.8053	0.0522	0.8209	0.4707	0.0092	0.0077	0.0084	0.0363
3.2024	0.5663	0.01	0.045	0.0837	0.05325	866.5909	0.596	0.047	0.3038	0.1363	0.0143	0.0151	0.0124	0.0806
12.8098	9.0611	0.025	0.045	0.1323	0.70135	3424.432	1.6499	0.098	3.3637	1.9699	0.0066	0.0072	0.0071	0.0268
9.6073	5.0968	0.025	0.045	0.1323	0.445	3424.432	1.4725	0.0938	2.2515	1.1790	0.0078	0.0086	0.0081	0.0342
6.4049	2.2653	0.025	0.045	0.1323	0.22375	3424.432	1.2539	0.0897	1.2782	0.5604	0.0112	0.0118	0.0102	0.051
3.2024	0.5663	0.025	0.045	0.1323	0.06465	3424.432	0.9255	0.0851	0.4717	0.1520	0.0244	0.0242	0.0169	0.1377

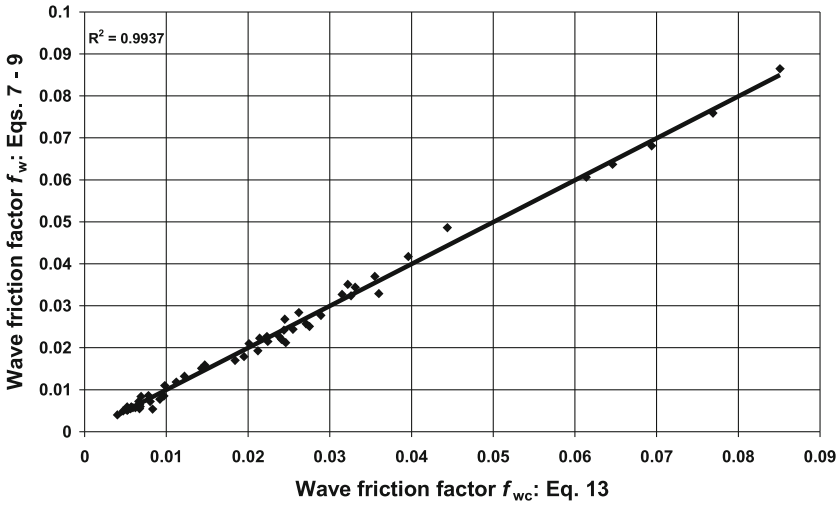

Fig. 1 Wave friction factors given by Eqs. 7–9 plotted against Eq. 3 for smooth, transitional and rough boundary conditions

which has an R^2 value of 0.9938 compared to 0.8638 of Eq. 10. In the case of Wang (2007), however, the values of f_w are greatly underestimated and there is hardly any increase in the calculated value of Eq. 11 with respect to Eq. 3.

For rough boundary conditions, numerous equations have also been proposed. For example, Jonsson (1963) used

$$f_w = \frac{0.0604}{\log\left(\frac{30\delta}{D}\right)^2} \tag{12}$$

Swart and Fleming (1980) proposed the following formulae:

for $7<\frac{A_{wb}}{D}<160$

$$f_w = 0.00066 + 0.483\left(\frac{A_{wb}}{D}\right)^{-0.91} \tag{13}$$

and for $160<\frac{A_{wb}}{D}$

$$f_w = 0.0146\left(\frac{A_{wb}}{D}\right)^{-0.157} + 0.483\left(\frac{A_{wb}}{D}\right)^{-0.91} \tag{14}$$

Figure 3 plots the values given by Eqs. 9, 12 and 13–14 against those of Eq. 3. In the case of Jonsson (1963), δ was here calculated using the method proposed by Le Roux (2010b). As shown in Fig. 3, Eqs. 9 and 12 coincide reasonably well between f_w values of 0.005 and 0.015, but for higher values of f_w, Jonsson (1963) appears to deviate sharply from Eq. 3. The equations of Swart and Fleming (1980) greatly overestimate the value given by Eq. 3.

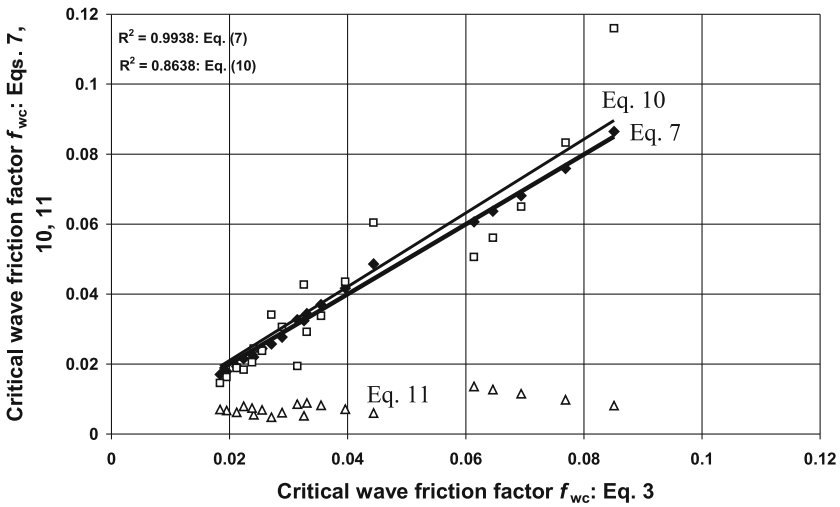

Fig. 2 Wave friction factors given by Eqs. 7, 10, and 11 plotted against Eq. 3 for smooth (laminar) boundary conditions

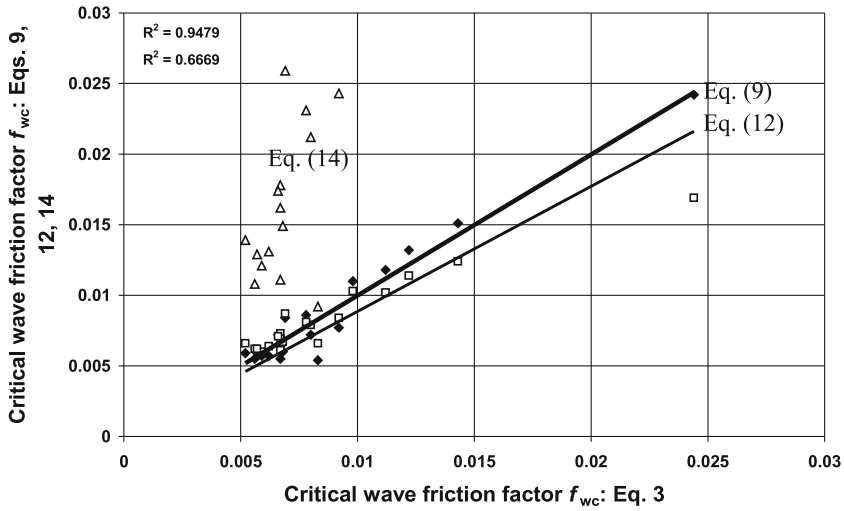

Fig. 3 Wave friction factors given by Eqs. 9, 12, and 14 plotted against Eq. 3 for rough (turbulent) boundary conditions

Discussion

From the comparisons above, it appears that those equations using the water particle semi-excursion at the top of the boundary layer, A_{wb}, yield results deviating sharply from the wave friction factor as calculated by Eq. 3. This is probably because A_{wb} is commonly determined from linear wave theory using the equation

$$A_{wb} = \frac{U_{wb} T_w}{2\pi} \tag{15}$$

However, it can be shown that Eq. 15 is in fact no longer valid at the top of the boundary layer. Le Roux (2010b) calculated the horizontal semi-excursion A_{whz} for any depth z below the displaced mean water level DWL (Le Roux 2008a) by

$$A_{whz} = \frac{H_o}{2} \frac{\cosh\left(\frac{\pi d - z}{MCD_w}\right)}{\cosh\left(\frac{\pi d}{MCD_w}\right)} \tag{16}$$

where MCD_w is the mean crest diameter in any water depth (Le Roux 2008b). Setting $z=d$ gives the horizontal semi-excursion at the top of the boundary layer A_{wb}. At the DWL ($z=0$) itself, Eqs. 15 and 16 give the same results, but at the top of the boundary layer under linear (deepwater) wave conditions, A_{wb} as determined by Eq. 15 is half the value given by Eq. 16.

The vertical semi-excursion A_{wvz} at any depth z is found by (Le Roux 2010b; Le Roux et al. 2010)

$$A_{wvz} = \frac{H_o}{2} \frac{\sinh\left(\frac{\pi d - z}{MCD_w}\right)}{\sinh\left(\frac{\pi d}{MCD_w}\right)} \tag{17}$$

which reduces to zero at the top of the boundary layer.

The difference between these models has important implications with regard to the general consensus that water particle motion in deep water is circular right down to the bottom, and that the decrease of the orbital diameter d_o with depth below the surface is in accordance with the standard Airy (1845) equation:

$$d_o = H_o \exp\left(\frac{-\pi dz}{L_o}\right) \tag{18}$$

where L_o is the deepwater wavelength.

This principle has been incorporated in most, if not all, linear wave models and equations. However, there is a conceptual problem with Eq. 18, as shown in Fig. 4. The center of the circular orbit coincides with the DWL at the surface, but at a depth of $z=d$ below the latter it must lie just above the bottom itself. Using the first case in Table 1 as an example (a 12.8 s wave propagating at 163 m depth, thus defining deepwater conditions according to the currently accepted limit of $\frac{L_o}{2}$), the boundary layer is only 0.045 cm thick. However, the orbital diameter is 16.64 cm at this depth. Therefore, 8.28 cm of the circular orbit must lie below the sediment surface, which is clearly impossible.

Equations 16 and 17 also model circular orbits near the surface, where both $2A_{whz}$ and $2A_{wvz}$ correspond exactly to d_o as given by Eq. 18. Up to a distance of about $\frac{L_o}{2}$ from the surface, the value of $2A_{whz}$ deviates less than 5% from d_o, but from this level it begins to diverge increasingly until it reaches exactly $2d_o$ at the top of the boundary layer, where $2A_{wvz}$ reduces to zero (Fig. 4). This should be so, because the water particle motion in the boundary layer by definition must be only to-and-fro. Furthermore, because the particles accelerate from zero to a maximum below the passing wave crest and back to zero at the arrival of the trough, and since the acceleration and deceleration are uniform and along a straight line, the maximum velocity must be twice the mean velocity. The latter is given by $\frac{2\pi d_o}{T_w}$, i.e., at a depth of 163 m for a 12.8 s wave it would be

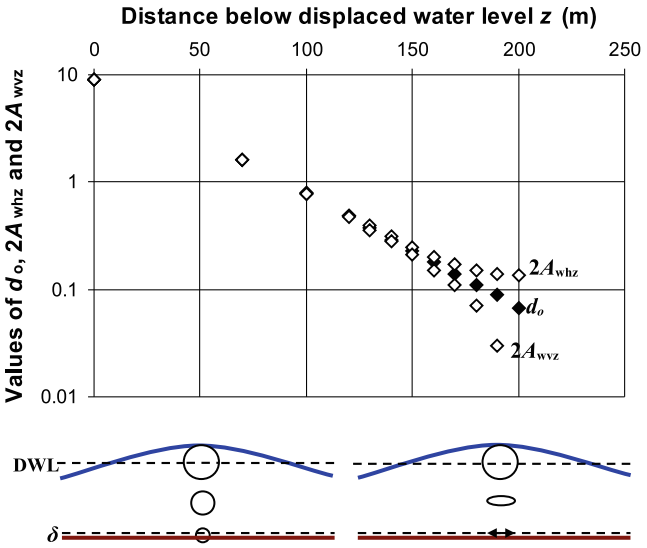

Fig. 4 Model of water particle motion for the specific case of a 12.8 s wave propagating in deep water, showing how vertical ($2A_{wvz}$) and horizontal ($2A_{whz}$) water particle excursions change with depth as compared to orbital diameter (d_o). *Bottom left* Traditional model of water particle motion, *bottom right* model proposed here

4.08 cm s^{-1}. This is modeled correctly by the equation of Le Roux (2010b):

$$U_{wb} = \frac{gT_w H_o L_w}{4MCD_w^2} \tag{19}$$

where L_w is the wavelength in any water depth. This yields a maximum boundary velocity of 8.16 cm s^{-1} under the wave crest. It is therefore proposed that Eqs. 17 and 18 be used instead of Eq. 15 to calculate horizontal and vertical water particle semi-excursions at any depth below the surface, and particularly for the top of the boundary layer. These equations also have the advantage that they are valid for both linear and non-linear wave conditions.

Conclusions

The fact that U_{wb} as determined by Eq. 19 and employed in Eqs. 7 and 9 yields wave friction factors similar to those given by Jonsson (1963, 1966) and Schlichting (1968) not only supports the model of water particle motion shown in Fig. 4, but also suggests that Eqs. 7–9 can be used with confidence to predict sediment transport in conjunction with the maximum and critical wave boundary velocity.

As shown in WAVECALC II, for a 12.81 s wave, entrainment of 0.01 mm grains should commence at a depth of about 163 m, when the maximum boundary velocity under the wave crest begins to exceed the critical boundary velocity. However, the wave friction factor only exceeds the critical wave friction factor at a depth of about 147 m. On the other hand, for a 10 mm grain under the same wave conditions, entrainment according to the wave friction factor would take place at a depth of 56 m, compared to 55 m using the maximum boundary velocity. This is because of an additional force related to the pressure gradient under waves, which increases into shallow water (Le Roux 2010a). Although both methods may therefore be employed to predict sediment entrainment, the wave friction factor has the added advantage that it can be used in combination with unidirectional currents.

Acknowledgements I am grateful to three anonymous reviewers and the editors for their valuable comments that helped to improve the paper.

Appendix 1

Equations used to determine sediment entrainment by traction (Le Roux 1992; 1998)

$$U_{*_c} = \sqrt{\frac{gD\rho_\gamma \tau_{dc}}{\rho}} \tag{1}$$

$$\tau_{dc} = -0.717\log_{10} W_d + 0.0625 = \text{for } W_d < 2.5 \tag{2}$$
$$\tau_{dc} = 0.0171\log_{10} W_d + 0.0272 \text{ for } 2.5 < W_d < 11$$
$$\tau_{dc} = 0.045 \text{ for } W_d > 11$$

$$W_d = (0.2354 D_d)^2 \text{ for } D_d < 1.2538 \tag{3}$$
$$W_d = (0.208 D_d - 0.0652)^{3/2} \text{for } 1.2538 < D_d < 2.9074$$
$$W_d = (0.2636 D_d - 0.37) \text{for } 2.9074 < D_d < 22.9866$$
$$W_d = (0.8255 D_d - 5.4)^{2/3} \text{ for } 22.9866 < D_d < 134.9215$$
$$W_d = (2.531 D_d + 160)^{1/2} \text{ for } 134.9215 < D_d < 1750$$

$$W_d = W_3 \sqrt{\frac{\rho^2}{g\mu\rho_\gamma}} \tag{4}$$

$$D_d = D_3 \sqrt{\frac{g\rho\rho_\gamma}{\mu^2}} \tag{5}$$

Appendix 2

List of symbols

A_{wb}	horizontal water particle semi-excursion at top of boundary layer
A_{whz}	horizontal water particle semi-excursion at any depth z below DWL
A_{wvz}	vertical water particle semi-excursion at any depth z below DWL
d	water depth
d_o	orbital diameter

d_{ob}	orbital diameter at top of boundary layer
D	median grain size
D_d	dimensionless median grain size
DWL	displaced water depth
f_w	wave friction factor
f_{wc}	critical wave friction factor
g	acceleration due to gravity
H_o	fully developed deepwater wave height
L	length
L_o	deepwater wavelength
L_w	wavelength in any water depth
MCD_w	median crest diameter in any water depth
P_w	horizontal pressure force across grain under waves
Re	Reynolds number
Re_{*c}	boundary Reynolds number
SWL	still water level
T_w	wave period
U	velocity
U_{wb}	boundary velocity
U_{wbc}	critical boundary velocity
U_{wi}	instantaneous velocity
U_*	shear velocity
U_{*c}	critical shear velocity required to entrain sediments under unidirectional currents
U_{*wc}	critical wave boundary shear velocity under wave crest
W_d	dimensionless settling velocity
z	depth below DWL
zb	vertical coordinate measured upwards from bed
δ	thickness of boundary layer
μ	dynamic water viscosity
ρ	water density
ρ_γ	submerged sediment density (grain density minus water density)
τ_c	critical shear stress
τ_t	total shear stress
τ_u	current-induced shear stress
τ_w	wave-induced shear stress (oscillatory shear stress)
τ_{wc}	critical shear stress under waves
τ_{dc}	dimensionless critical shear stress (Shields 1936)
υ_t	turbulent eddy viscosity
ω	radian frequency

References

Airy GB (1845) Tides and waves. Encyc Metrop Article 192:241–396

Aydin I, Shuto N (1998) An application of the k-epsilon model to oscillatory boundary layers. Coastal Eng Jpn 30:11–24

Hsu T, Ou S (1997) Wave boundary layers in rough turbulent flow. J Coastal Eng 24:25–43

Jonsson IG (1963) Measurements in the turbulent wave boundary layer. In: Proc 10th Congr, IAHR, London, vol 1, pp 85–92

Jonsson IG (1966) Wave boundary layer and friction factors. In: Proc 10th Int Conf Coastal Engineering, ASCE, Tokyo, vol 1, pp 127–148

Justesen P (1988) Prediction of turbulent oscillatory flow over rough beds. Coastal Eng 12:257–284

Komar PD, Miller MC (1973) The threshold of sediment movement under oscillatory water waves. J Sedim Petrol 4:1101–1110

Le Roux JP (1992) Settling velocity of spheres: a new approach. Sedim Geol 81:11–16

Le Roux JP (1998) Entrainment thresholds of natural grains in liquids determined empirically from dimensionless settling velocities and other measures of grain size. Sedim Geol 119:17–23

Le Roux JP (2003) Wave friction factor as related to the Shields parameter for steady currents. Sedim Geol 155:37–43

Le Roux JP (2008a) Profiles of fully developed (Airy) waves in any water depth. Coastal Eng 55:701–703

Le Roux JP (2008b) An extension of the Airy theory for linear waves into shallow water. Coastal Eng 55:295–301

Le Roux JP (2010a) A comparison of velocity profiles in unidirectional currents and the wave boundary layer: implications for sediment entrainment. Sedim Geol 232:84–90

Le Roux JP (2010b) Sediment entrainment under fully developed waves as a function of water depth, boundary layer thickness, bottom slope and roughness. Sedim Geol 223:143–149

Le Roux JP, Demirbilek Z, Brodalka M, Flemming BW (2010) WAVECALC: an Excel-VBA spreadsheet to model the characteristics of fully developed waves and their influence on bottom sediments in different water depths. Geo-Mar Lett 30(5):549–560. doi:10.1007/s00367-010-0195-x

Mirfenderesk H, Young IR (2003) Direct measurements of the bottom friction factor beneath surface gravity waves. Appl Ocean Res 25:269–287

Schlichting H (1968) Boundary layer theory, 6th edn. McGraw-Hill, New York

Shields A (1936) Anwendung der Ähnlichkeitsmechanik und der Turbulenzforschung auf die Geschiebebewegung. Mitteilungen der Preussischen Versuchsanstalt für Wasser-, Erd- und Schiffbau, Berlin, no 26

Soulsby RL, Whitehouse RJS (1997) Threshold of sediment motion in coastal environments. In: Proc Pacific Coasts and Ports 1997. 13th Australasian Coastal and Engineering Conf and 6th Australian Port and Harbour Conf, Christchurch, New Zealand. HR Wallington, Oxon, pp 149–154

Swart DH, Fleming CA (1980) Long shore water and sediment movement. In: Proc 17th Int Conf Coastal Engineering, ASCE, Sydney, vol 2, pp 1275–1294

Teleki PG (1972) Wave boundary layers and their relation to sediment transport. In: Swift DJP, Duane DB, Pilkey OH (eds) Shelf sediment transport: process and pattern. Dowden, Hutchinson and Ross, Stroudsburg, PA, pp 21–59

Trowbridge J, Madsen OS (1984a) Turbulent wave boundary layers. Model formulation and first order solution. J Geophys Res 89:7989–7997

Trowbridge J, Madsen OS (1984b) Turbulent wave boundary layers 2. Second order theory and mass transport. J Geophys Res 89:7999–8007

Wang Y-H (2007) Formula for predicting bedload transport rate in oscillatory sheet flows. Coastal Eng 54:594–601

You ZJ, Wilkinson DL, Nielsen P (1992) Velocity distribution in turbulent oscillatory boundary layer. Coastal Eng 18:21–38